High-Efficiency Dye-Sensitized Solar Cells: The Influence of Lithium Ions on Exciton Dissociation, Charge Recombination, and Surface States

ARTICLE *in* ACS NANO · OCTOBER 2010

Impact Factor: 12.88 · DOI: 10.1021/nn101384e · Source: PubMed

7 AUTHORS, INCLUDING:

Qingjiang Yu
Harbin Institute of Technology
65 PUBLICATIONS **2,342** CITATIONS
SEE PROFILE

Jing Zhang
Fourth Military Medical University
689 PUBLICATIONS **10,054** CITATIONS
SEE PROFILE

Min Zhang
Chinese Academy of Sciences
39 PUBLICATIONS **2,147** CITATIONS
SEE PROFILE

Peng Wang
Beijing University of Civil Engineering and …
748 PUBLICATIONS **18,077** CITATIONS
SEE PROFILE

ARTICLE

High-Efficiency Dye-Sensitized Solar Cells: The Influence of Lithium Ions on Exciton Dissociation, Charge Recombination, and Surface States

Qingjiang Yu, Yinghui Wang, Zhihui Yi, Ningning Zu, Jing Zhang, Min Zhang, and Peng Wang*

State Key Laboratory of Polymer Physics and Chemistry, Changchun Institute of Applied Chemistry, Chinese Academy of Sciences, Changchun 130022, China

ABSTRACT We present a time-saving staining protocol based upon the low-toxicity and nonvolatile solvent dimethyl sulfoxide for a high-efficiency dye-sensitized solar cell, which is very critical for the roll-to-roll flexible cell production. Power conversion efficiencies of 11.7—12.1% were achieved under AM1.5G simulated sunlights. The intrinsic roles of lithium cations on efficiency enhancement were scrutinized by measuring transient absorption and electrical impedance spectroscopies. Our studies have revealed that lithium ions can enhance exciton dissociation at the energy-offset dye/titania interface effectively. Charge collection is not found to be a crucial current loss channel in our high-efficiency dye-sensitized solar cell.

KEYWORDS: solar cells · exciton dissociation · charge recombination · surface states · transient absorption spectroscopy · impedance spectroscopy

The mesoscopic dye-sensitized solar cell (DSC) is emerging as a promising thin-film photovoltaic device with an excellent price/performance ratio for the coming low-carbon energy supply.[1,2] A small-area lab testing cell showing ~11% efficiency measured at the 100 mW cm^{-2} AM1.5G conditions could be thus far fabricated based upon several polypyridyl ruthenium chromophores.[3−7] Note that the assembling of these cells all involved a time-consuming process, that is, an overnight dyeing of nanocrystalline titania films in solutions mainly composed of toxic and volatile acetonitrile, which is difficult to be integrated with the roll-to-roll flexible DSC production line.[8]

In this context a swift staining mode was thereby proposed on the basis of a high-concentration dye solution in toxic dimethylformide or methoxypropionitrile, but unfortunately generated a relatively poor cell efficiency of ~10%.[3] We herein identify the low-toxicity and nonvolatile solvent dimethyl sulfoxide (DMSO)[9,10] for a speedy dye-coating and demonstrate a DSC exhibiting an impressive efficiency of 11.7%, measured under 100 mW cm^{-2} AM1.5G sunlight. With the aid of transient absorption measurements, we have proven that the presence of lithium ions in the electrolyte can enhance the yield of exciton dissociation at the dye/titania interface, leading to a high photocurrent.

*Address correspondence to peng.wang@ciac.jl.cn.

Received for review June 19, 2010 and accepted September 28, 2010.

Published online October 5, 2010.
10.1021/nn101384e

RESULTS AND DISCUSSION

A double-layer titania film was used as the negative electrode of a DSC. A 15-μm-thick transparent layer of 20-nm-sized titania particles was first screen-printed onto a precleaned fluorine-doped tin oxide (FTO) conducting glass electrode (Nippon Sheet Glass, Solar, 4 mm thick), and subsequently coated by a 6-μm-thick second layer of scattering titania particles (WERO-4, Dyesol). The detailed preparation procedures of titania nanocrystals, pastes for screen-printing, and nanostructured titania films were reported previously.[11−13] A circular titania electrode (~0.28 cm^2) was stained in a DMSO solution (10 mM C106 dye as shown in Figure 1A and 10 mM chenodeoxycholic acid coadsorbent) for 5 min. The dye-coated titania electrode was subsequently washed with DMSO and ethanol in turn and then assembled with a thermally platinized FTO positive electrode (TEC 15 Ω/□, Libbey-Owens-Ford Industries, 2.2 mm thick). We note here that the operation with DMSO should be done with special care to avoid skin contact, since this solvent could penetrate skin easily, despite that it exhibits quite low toxicity. The two active electrodes were separated with a 30-μm-thick Bynel (DuPont) hot-melt gasket and sealed up by heating. The internal space was filled with a liquid electrolyte using a vacuum backfilling system. The electrolyte-injecting hole on the positive electrode, which was pre-

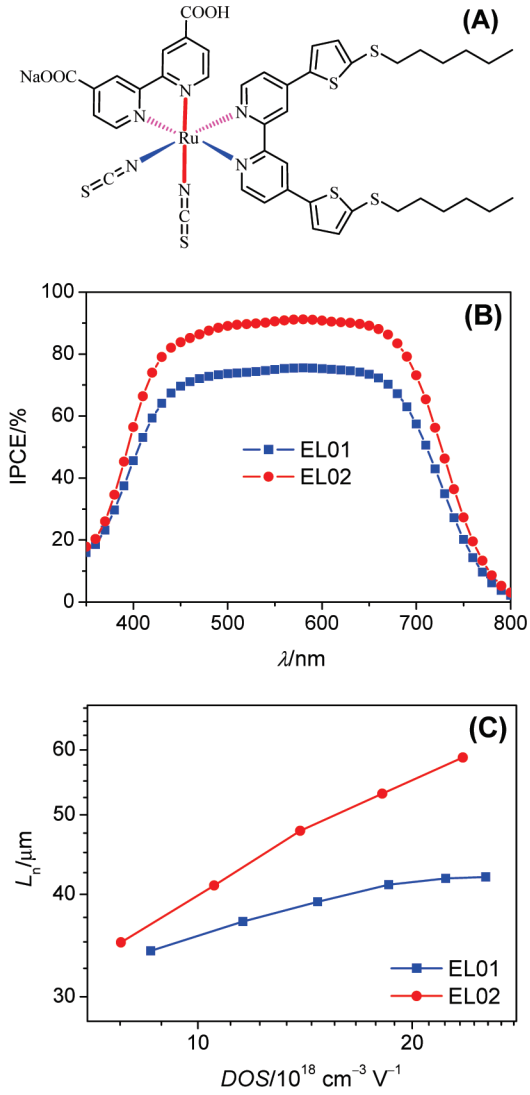

Figure 1. (A) Molecular structure of C106. (B) Photocurrent action spectra of C106 in conjunction with electrolytes EL01 and EL02. Cells were tested using a metal mask with an aperture area of 0.158 cm^2. An antireflection film was adhered to cells during measurements. (C) Plots of electron diffusion length *versus* density of states (DOS) derived from electrical impedance measurements.

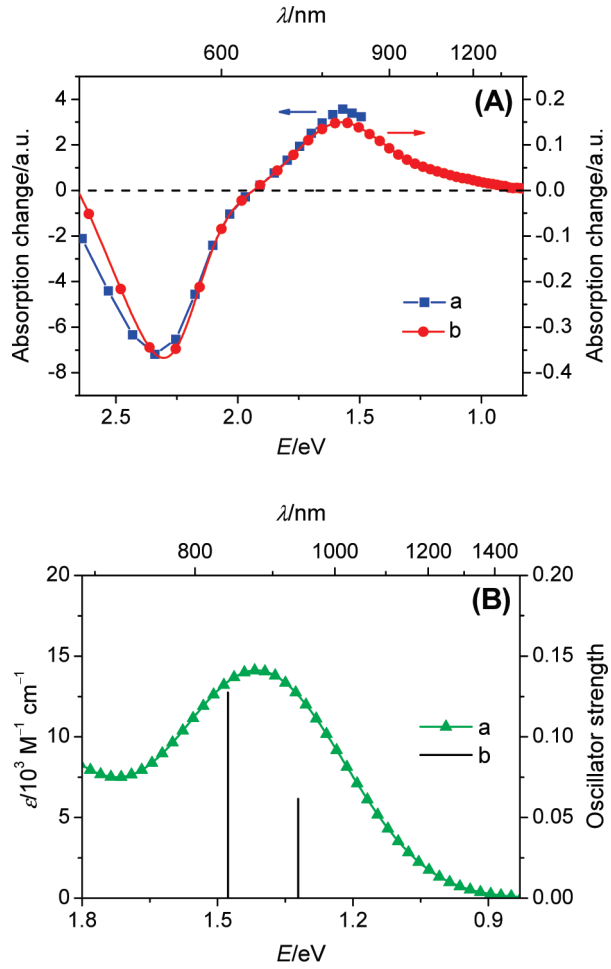

Figure 2. (A) Transient absorption change (a) recorded at 160 ns upon nanosecond pulsed 580 nm laser excitation of a C106-coated titania film immersed in the 85/15 mixed solvent of AN and VN, and absorption change (b) after applying a positive bias of 435 mV (*vs* Fc$^+$/Fc) to a C106-coated titania film immersed in EMITFSI. (B) Calculated electronic absorption spectrum (a) and oscillator strength (b) of the oxidized species of C106 tethered with hydroxylated titanium.

pared in advance with a sand-blasting drill, was sealed with a Bynel sheet and a thin glass cover by heating. Two electrolytes were used for device fabrication: EL01 consisting of 1.0 M 1,3-dimethylimidazolium (DMII), 30 mM iodine (I_2), 1.0 M 4-*tert*-butylpyridine (TBP), and 0.1 M guanidinium thiocyanate (GNCS) in the 85/15 mixture of acetonitrile (AN) and valeronitrile (VN); EL02 consisting of 1.0 M DMII, 50 mM LiI, 30 mM I_2, 1.0 M TBP, and 0.1 M GNCS in the 85/15 mixture of AN and VN. The mere difference between these two electrolytes is whether the lithium cation is included.

Photocurrent action spectra (Figure 1B) were first measured to roughly evaluate our cells in terms of an overall efficiency of light absorption, net charge generation, and charge collection. Both electrolytes confer a broad plateau of monochromatic incident photon-to-collected electron conversion efficiencies (IPCEs) onto the swiftly dye-coated titania film, implying a saturated light harvesting in this wavelength region. This scenario is closely related to the high molar absorption coefficient of C106 (18.7 × 10^3 M^{-1} cm^{-1} at 550 nm),[6] and the employment of a thick bilayer titania film, characteristic of a fairly large surface area[1,11−13] and a light-scattering function.[14−19] However, the IPCE summits are remarkably dissimilar for cells with EL01 and EL02, being ~75% and ~90%, respectively, even if identical dye-coated films are applied. In addition, no noticeable variation was perceived for their normalized photocurrent action spectra (Figure S1 of Supporting Information), suggesting that the charge collection may not be a prominent current loss channel in our cells. The charge collection yield was further evaluated with the electron diffusion length derived from the electrical impedance spectroscopy measurements, through fitting the impedance spectra with an appropriate equiva-

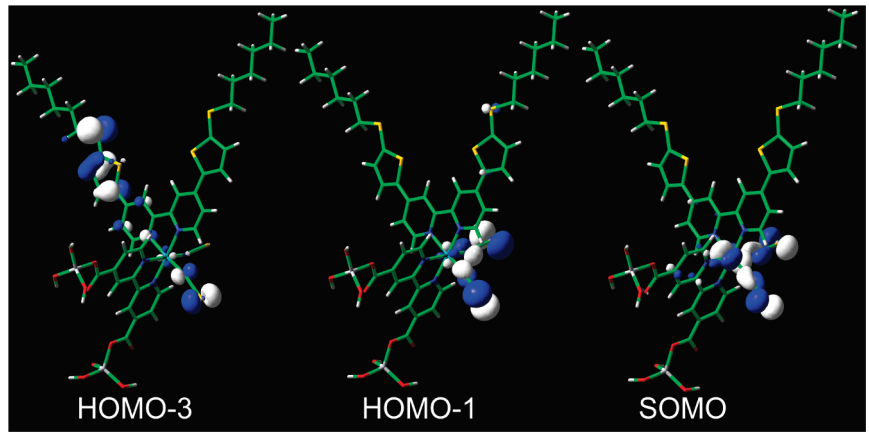

Figure 3. Contour plots of transition-involved frontier molecular orbitals of the oxidized species of C106 tethered with hydroxylated titanium. All the isodensity surface values are fixed at 0.04.

lent electrical circuit[20] adaptable to DSCs. As clarified in Figure 1C, the electron diffusion lengths are actually over 34 μm in these two cells and much larger than the nanoporous titania film thickness of 15 μm.

The intrinsic origins of IPCE height difference in the preceding observations were elaborated through laser-induced transient absorption measurements. Upon the 580-nm laser excitation of a 5-μm-thick C106-coated transparent titania film in contact with an inactive 85/15 mixture of AN and VN, we first recorded a transient absorption spectrum (trace a in Figure 2A) at 160 ns using a white probe light. A broad negative feature arises in the visible region between 2.65 and 1.91 eV, which could be allocated to the photobleaching of ground-state dye molecules, considering the absorption profile of a dye-coated film measured by a steady-state UV−visible spectrometer (Figure S2 of Supporting Information). With the aid of the spectroelectrochemical measurement (trace b in Figure 2A) on a C106-coated film immersed in 1-ethyl-3-methylimidazolium bis(trifluoromethanesulfonyl)imide (EMITFSI), we can unambiguously ascribe the positive signal in the transient absorption spectrum to electronic excitations of oxidized dye cations. Note that the concomitant electrons in titania upon laser excitation exhibit relatively weak absorptions throughout this spectral region, with an absorption coefficient of ~3400 M^{-1} cm^{-1} at 780 nm.[21] Generally, the transient spectrum probed for C106 is similar to those reported for other ruthenium sensitizers.[22−25]

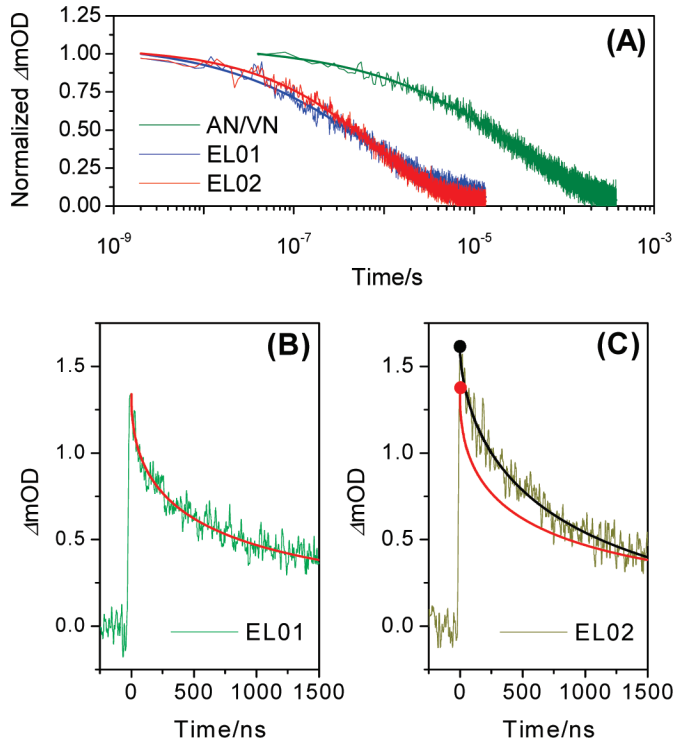

Figure 4. (A) Time-resolved absorption traces of C106-coated titania films immersed in the 85/15 mixture of AN and VN, and electrolytes. (B) Absorption trace with electrolyte EL01 in the nanosecond time domain. (C) Absorption trace with electrolyte EL02 in the nanosecond time domain. Absorbance changes were measured at a probe wavelength of 780 nm upon 440 nm laser excitation (7 ns full width half-maximum pulse duration, 2 Hz repetition rate, 78 μJ cm^{-2} pulse fluence). Smooth lines are stretched exponential fittings over raw data obtained by averaging 1600 laser shots. The red fitting line over the raw data with EL01 in panel B is also included in panel C for comparison. The red and black dots in panel C represent the initial fitting amplitudes in the cases of EL01and EL02, respectively.

To gain a mechanism insight into the transition characteristics of oxidized dye cations, we performed density functional theory (DFT) and time-dependent density functional theory (TDDFT)[26,27] calculations using the Gaussian 03 program package. Figure 2B displays the calculated absorption spectrum in the infrared region of the oxidized species of C106 tethered with hydroxylated titanium. The featureless absorption band mainly stems from the electron transition at 1.32 eV from HOMO−1 (HOMO is the highest occupied molecular orbital) to the singly occupied molecular orbital (SOMO), and that at 1.48 eV from HOMO−3 to SOMO. A close look on the isodensity plots of these frontier orbitals illustrated in Figure 3 discloses that the ligand-to-metal charge transfer (LMCT) transitions arise from the thiocyanate ligand and the 4,4′-bis(5-

(hexylthio)thiophen-2-yl)-2,2′-bipyridine ancillary ligand to the Ru(III) center.

On the basis of transient absorption spectrum and spectroelectrochemical measurements, we selected a monochromatic light at 780 nm to probe the multichannel charge transfer kinetics of oxidized dye cations. Excitation fluence was carefully controlled in our kinetic measurements to ensure that $\sim 1.57 \times 10^{14}$ photons cm^{-2} were absorbed by the dye-coated film during every laser pulse, which is close to the device operation condition. In the absence of a redox mediator (*i.e.*, in the inactive 85/15 mixture of AN and VN), the decay of absorption signals (Figure 4A) could be attributed to the back electron transfer from titania to oxidized dye cations and well fitted to a stretched exponential decay function ($\Delta OD \propto \exp[-(t/\tau)^{\alpha}]$), featuring a typical half-reaction time ($t_{1/2}$) of 15.5 μs. In the presence of iodide/triiodide redox electrolytes EL01 and EL02, the decay of oxidized dye absorption was significantly accelerated. For electrolyte EL01, the half-reaction time ($t_{1/2}$ = 0.41 μs) of the dye regeneration process is very close to that obtained with electrolyte EL02 ($t_{1/2}$ = 0.47 μs). The alike branching ratios of back charge transfer and dye regeneration in both electrolytes are over 33, showing that more than 97% of oxidized dyes are intercepted *via* the electron donation from iodide. We therefore conclude that the difference in the kinetic competition between these two charge-transfer channels does not make a significant contribution to the aforementioned IPCE height discrepancy.

We further scrutinized the exciton dissociation yield by means of measuring the initial amplitudes[28,29] of oxidized dye cations in the cases of electrolytes EL01 and EL02, while the dye-coated films absorb the same number of photons. Smooth red and black curves presented in Figure 4B,C are the corresponding fittings over absorption traces of oxidized dye cations in the presence of electrolytes EL01 and EL02, respectively. As depicted in Figure 4C, the initial amplitude of oxidized dye cation absorption with EL02 is evidently (by ~15%) higher than that with EL01, soundly explaining the observed IPCE height difference. The favorable role of lithium ions on exciton dissociation was also previously noted for other photosensitizers.[24,30−33] Since the energy difference between the LUMO of C106 and the conduction band edge of titania is ~0.62 eV,[6] we deduce that the improvement on electron injection efficiency in our case might be ascribed to the interfacial dipole assisting exciton dissociation,[34,35] owing to the adsorption of lithium ions on titania nanocrystals.

J−*V* characteristics of both cells measured under an irradiation of AM1.5G full sunlight are presented in Figure 5A. The short-circuit photocurrent density (J_{sc}),

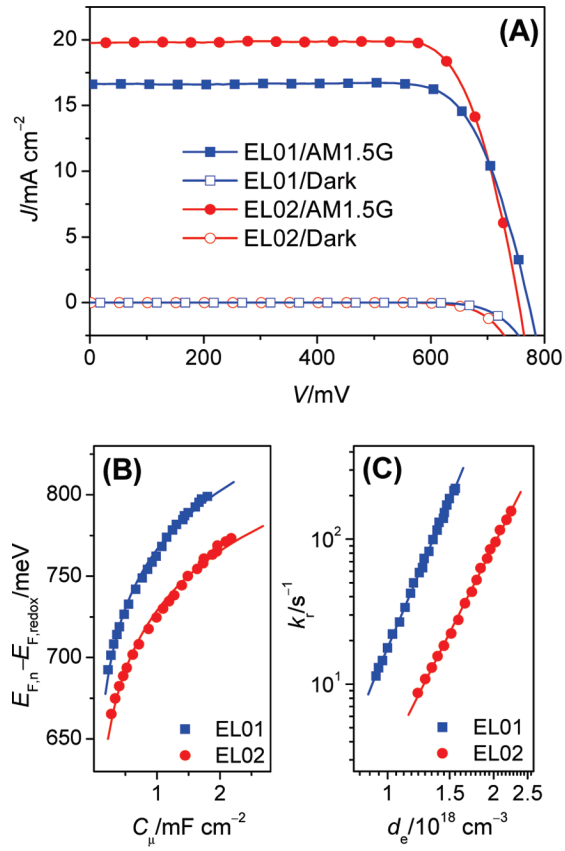

Figure 5. (A) *J*−*V* characteristics of C106 in combination with electrolytes EL01 and EL02 measured under irradiation of 100 mW cm^{-2} AM1.5G sunlight. Cells were tested using a metal mask with an aperture area of 0.158 cm^2. An antireflection film was adhered to cells during measurements. (B) Chemical capacitance and (C) charge recombination rate constant measured by transient photoelectric decays.

open-circuit photovoltage (V_{oc}), and fill factor (FF) of a cell with electrolyte EL01 are 16.62 mA cm^{-2}, 774 mV, and 0.767, respectively, yielding an overall conversion efficiency (η) of 9.9%. In contrast, the photovoltaic parameters (J_{sc}, V_{oc}, FF, and η) of a cell with electrolyte EL02 are 19.78 mA cm^{-2}, 758 mV, 0.779, and 11.7%, respectively. The photocurrent tendency of EL02 with respect to EL01 is in good accord with that observed in IPCE measurements. In view that DSC is a very promising candidate for the conversion of weak light to electricity,[2] we also measured cell efficiencies by attenuating the AM1.5G full sunlight with a set of neutral metal meshes, and detailed cell parameters are collected in Table 1. At a light intensity of 26.14 mW cm^{-2}, the cell performance is pretty impressive, reaching an efficiency of 12.1%.

To comprehend the adverse effect of lithium ions on the cell photovoltage (EL02 versus EL01, Figure 5A), we resorted to the transient photoelectric decay technique[37−40] to measure the charge recombination rate constant (k_r) at the titania/electrolyte interface as well as the interfacial chemical capacitance (C_μ). The latter is closely related to density of surface states on titania nanocrystals. As shown in Figure 5B, at a given

TABLE 1. Detailed Photovoltaic Parameters of C106 with EL02 Measured at a Set of Incident Light Intensities[a]

P_{in} (mW cm^{-2})	J_{sc} (mA cm^{-2})	V_{oc} (mV)	FF	η (%)
14.39	2.86	704	0.837	11.7
26.14	5.26	721	0.834	12.1
53.26	10.63	740	0.810	12.0
100	19.78	758	0.779	11.7

[a]The spectral distribution of our light resource simulates AM1.5G solar emission with a mismatch less than 4%. Lights at different intensities were obtained by attenuating the AM1.5G full sunlight with a set of neutral meshes. Incident power intensity, P_{in}; short-circuit photocurrent density, J_{sc}; open-circuit photovoltage, V_{oc}; fill factor, FF; total power conversion efficiency, η. Cell area tested with a metal mask: 0.158 cm^2. An antireflection film was adhered to testing cells during measurements. EL02: 1.0 M DMII, 50 mM LiI, 30 mM I_2, 1.0 M TBP, and 0.1 M GNCS in a 85/15 mixture of AN and VN.

Fermi-level difference ($E_{F,n} - E_{F,redox}$), the C_μ with EL02 is apparently larger than that with EL01, which is well consistent with the notion that the addition of lithium ions can lead to more deep surface states below the conduction band edge.[41] More deep states tends to lower the $E_{F,n}$ at a given electron injection rate. Also, the adsorption of lithium cations is known to noticeably downward displace the titania conduction band edge (E_c) relative to the electrolyte Fermi level ($E_{F,redox}$),[24] probably through inducing a surface dipole pointing from the titania to electrolyte. This downward E_c movement could adversely impact the photovoltage. Additionally, it can be easily perceived from Figure 5C that in comparison with EL01, the charge recombination rate (k_r) with EL02 is attenuated at a given electron density (d_e), in favor of a high cell photovoltage. Overall, the unfavorable surface state as well as the E_c effect of lithium ions overwhelms their advantageous influence on retarding the interfacial charge recombination, still resulting in a decreased photovoltage. Fortunately, the small loss of photovoltage in the presence of lithium ions is overcompensated by the photocurrent gain, leading to excellent power efficiencies for the conversion of solar power to electricity (Table 1).

SUMMARY

We have demonstrated a speedy staining protocol using a low-toxicity and nonvolatile solvent DMSO for the fabrication of a high-efficiency dye-sensitized solar cell, based upon the new-generation high-absorption-coefficient dye C106. Power conversion efficiencies of 11.7−12.1% were attained at the AM1.5G conditions. We anticipate that this discovery will benefit the roll-to-roll production of more efficient flexible dye-sensitized solar cells. We have also cautiously diagnosed the intrinsic role of lithium ions on efficiency enhancement through systematic photophysical and electrical characterizations. Our studies have shown that lithium ions can promote exciton dissociation at the energy-offset dye/titania interface effectively. In addition, charge collection is not found to be a crucial current loss channel in our high-efficiency dye-sensitized solar cell.

METHODS

Computational Details. The oxidized species of C106 tethered with hydroxylated titanium treated as an open-shell system was computed using the UPBE0 method. In our calculations, the standard 6-31G(d, p) basis set, including diffuse and polarization functions, was used for S, N, O, C, and H atoms, and LANL2DZ (Los Alamos National Laboratory 2 double ζ) basis set for the transition metal Ru atom.[42] On the basis of the optimized geometry of the C106 cation, the electronic absorption spectrum was calculated by the TDDFT method at UPBE0/6-31G (d, p), LANL2DZ level.

Photovoltaic Characterization. A Keithley 2400 source meter and a Zolix Omni-λ300 monochromator equipped with a 500 W xenon lamp were used for photocurrent action spectrum measurements, with a wavelength sampling interval of 10 nm and a current sampling time of 2 s under the full computer control. Monochromatic incident photon-to-collected electron conversion efficiency (IPCE) is defined by $IPCE(\lambda) = hcJ_{sc}/(e\phi\lambda)$, where h is the Planck constant, c is the light speed in vacuum, e is the electronic charge, λ is the wavelength, J_{sc} is the short-circuit photocurrent density, and ϕ is the incident radiative flux. A Hamamatsu S1337-1010BQ silicon diode used for IPCE measurements was calibrated at the National Institute of Metrology, China. A model LS1000-4S-AM1.5G-1000W solar simulator (Solar Light Company, USA) in combination with a metal mesh was employed to give an irradiance of 100 mW cm^{-2}. The light intensity was tested with a PMA2144 pyranometer and a calibrated PMA 2100 dose control system. $J-V$ characteristics were obtained by applying a potential bias to a testing cell and measuring dark current and photocurrent with a Keithley 2602 source meter under the full computer control. The measurements were fully automated using Labview 8.0. A metal mask with an aperture area of 0.158 cm^2 was covered on a testing cell during all measurements. An antireflection film (λ < 380 nm, ARKTOP, ASAHI Glass) is adhered to the DSC photoanode during IPCE and $J-V$ measurements. The short-circuit photocurrent densities measured under this solar simulator are well consistent with the integral of IPCEs with the AM1.5G spectrum (ASTM G173−03), within a 4% error.

Transient Photoelectric Measurements. In transient photoelectric decay experiments, a steady light was supplied with a white light-emitting diode (LED) array while a perturbing light pulse was provided with a red LED array controlled by a fast solid-state switch. Both white and red lights were irradiated on the photoanode side of a testing cell. The red pulse was carefully controlled by the driving potential of diodes to keep the modulated photovoltage below 5 mV. We used red light as a probe to generate a photovoltage perturbation near the open-circuit photovoltage (V_{oc}) of the cell under the white light and measured the voltage decay process thereafter. Normally, the transient signals follow a monoexponential decay, thus the recombination rate constant, k_r, can be extracted from the slope of the semilogarithmic plot. The capacitance (C_μ) of the titania interface at the V_{oc} is calculated by $C_\mu = \Delta Q/\Delta V$, where ΔV is the peak of the photovoltage transient and ΔQ is the number of electrons injected during the red light flash. The latter is obtained by integrating a short-circuit photocurrent transient generated from an identical red pulse. The electron density (d_e) in the titania film under a given white light intensity was determined by a charge extraction technique.

Transient Absorption Measurements. Transient absorption measurements were carried out with a LP920 laser flash spectrometer in conjunction with a nanosecond tunable OPOLett-355II laser. The sample was kept at a 45° angle to the excitation beam. The probe light from a pulsed xenon arc lamp was passed through various optical elements, samples, and a monochroma-

tor before being detected by a fast photomultiplier tube and recorded with a TDS 3012C digital signal analyzer.

Electrical Impedance Spectroscopy Measurements. Electrical impedance experiments were performed under illumination of a red light-emitting diode on an IM6ex electrochemical workstation, with a frequency range from 50 mHz to 100 kHz and a potential modulation of 20 mV. A potential bias (V) was applied to equal the open-circuit photovoltage (V_{oc}) at each irradiation intensity, meeting the requirement of zero current. The obtained impedance spectra were fitted with the *Z*-view software (v2.80, Scribner Associates, Inc.).

Acknowledgment. We thank the National Key Scientific Program (No. 2007CB936700) and the CAS Knowledge Innovation Program (No. KGCX2-YW-326) for financial support. Q.Y. thanks the Postdoctoral Science Foundation of China (No. 20080440148). M.Z. thanks the State Key Laboratory of Theoretical and Computational Chemistry, Jilin University, for the computational resources. We are grateful to Dyesol for supplying the scattering paste and to DuPont Packaging and Industrial Polymers for supplying the Bynel film. We also thank Dr. K. Tabor from G24I for fruitful discussions.

Supporting Information Available: Normalized IPCE and absorption spectrum of the C106-coated titania film. This material is available free of charge via the Internet at http://pubs.acs.org.

REFERENCES AND NOTES

1. O'Regan, B.; Grätzal, M. A Low-Cost, High-Efficiency Solar Cell Based on Dye-Sensitized Colloid TiO_2 Films. *Nature* **1991**, *353*, 737–740.
2. Grätzal, M. Recent Advances in Sensitized Mesoscopic Solar Cells. *Acc. Chem. Res.* **2009**, *42*, 1788–1798.
3. Nazeeruddin, M. K.; De Angelis, F.; Fantacci, S.; Selloni, A.; Viscardi, G.; Liska, P.; Ito, S.; Takeru, B.; Grätzel, M. Combined Experimental and DFT−TDDFT Computational Study of Photoelectrochemical Cell Ruthenium Sensitizers. *J. Am. Chem. Soc.* **2005**, *127*, 16835–16847.
4. Chiba, Y.; Islam, A.; Watanabe, Y.; Komiya, R.; Koide, N.; Han, L. Dye-Sensitized Solar Cells with Conversion Efficiency of 11.1%. *Jpn. J. Appl. Phys., Part 2* **2006**, *45*, L638–L640.
5. Gao, F.; Wang, Y.; Shi, D.; Zhang, J.; Wang, M.; Jing, X.; Humphry-Baker, R.; Wang, P.; Zakeeruddin, S. M.; Grätzel, M. Enhance the Optical Absorptivity of Nanocrystalline TiO_2 Film with High Molar Extinction Coefficient Ruthenium Sensitizers for High Performance Dye-Sensitized Solar Cells. *J. Am. Chem. Soc.* **2008**, *130*, 10720–10728.
6. Cao, Y.; Bai, Y.; Yu, Q.; Cheng, Y.; Liu, S.; Shi, D.; Gao, F.; Wang, P. Dye-Sensitized Solar Cells with a High Absorptivity Ruthenium Sensitizer Featuring a 2-(Hexylthio)thiophene Conjugated Bipyridine. *J. Phys. Chem. C* **2009**, *113*, 6290–6297.
7. Chen, C.-Y.; Wang, M.; Li, J.-Y.; Pootrakulchote, N.; Alibabaei, C. N.; Decoppet, J.-D.; Tsai, J.-H.; Grätzel, C.; Wu, C.-G.; Zakeeruddin, S. M.; Grätzel, M. Highly Efficient Light-Harvesting Ruthenium Sensitizer for Thin-Film Dye-Sensitized Solar Cells. *ACS Nano* **2009**, *3*, 3103–3109.
8. G24 Innovations. http://www.g24i.com.
9. Willson, J. E.; Brown, D. E.; Timmens, E. K. A Toxicologic Study of Dimethyl Sulfoxide. *Toxicol. Appl. Pharmacol.* **1965**, *7*, 104–112.
10. Brayton, C. F. Dimethyl Sulfoxide (DMSO): A Review. *Cornell Vet.* **1986**, *76*, 61–90.
11. Brabé, C. J.; Arendse, F.; Comte, P.; Jirousek, M.; Lenzmann, F.; Shklover, V.; Grätzel, M. Nanocrystalline Titanium Oxide Electrodes for Photovoltaic Applications. *J. Am. Ceram. Soc.* **1997**, *80*, 3157–3171.
12. Wang, P.; Zakeeruddin, S. M.; Comte, P.; Charvet, R.; Humphry-Baker, R.; Grätzel, M. Enhance the Performance of Dye-Sensitized Solar Cells by Co-grafting Amphiphilic Sensitizer and Hexadecylmalonic Acid on TiO_2 Nanocrystals. *J. Phys. Chem. B* **2003**, *107*, 14336–14341.
13. Ito, S.; Murakami, T. N.; Comte, P.; Liska, P.; Grätzel, C.; Nazeeruddin, M. K.; Grätzel, M. Fabrication of Thin Film Dye Sensitized Solar Cells with Solar to Electric Power Conversion Efficiency over 10%. *Thin Solid Films* **2008**, *516*, 4613–4619.
14. Usami, A. Theoretical Study of Application of Multiple Scattering of Light to a Dye-Sensitized Nanocrystalline Photoelectrichemical Cell. *Chem. Phys. Lett.* **1997**, *277*, 105–108.
15. Ferber, J.; Luther, J. Computer Simulations of Light Scattering and Absorption in Dye-Sensitized Solar Cells. *Solar Energy Mater. Solar Cells* **1998**, *54*, 265–275.
16. Rothenberger, G.; Comte, P.; Grätzel, M. A Contribution to the Optical Design of Dye-Sensitized Nanocrystalline Solar Cells. *Solar Energy Mater. Solar Cells* **1999**, *58*, 321–336.
17. Wang, Z.-S.; Kawauchi, H.; Kashima, T.; Arakawa, H. Significant Influence of TiO_2 Photoelectrode Morphology on the Energy Conversion Efficiency of N719 Dye-Sensitized Solar Cell. *Coord. Chem. Rev.* **2004**, *248*, 1381–1389.
18. Hore, S.; Vetter, C.; Kern, R.; Smit, H.; Hinsch, A. Influence of Scattering Layers on Efficiency of Dye-Sensitized Solar Cells. *Solar Energy Mater. Solar Cells* **2006**, *90*, 1176–1188.
19. Koo, H.-J.; Park, J.; Yoo, B.; Yoo, K.; Kim, K.; Park, N.-G. Size-Dependent Scattering Efficiency in Dye-Sensitized Solar Cell. *Inorg. Chim. Acta* **2008**, *361*, 677–683.
20. Bisquert, J. Theory of the Impedance of Electron Diffusion and Recombination in a Thin Layer. *J. Phys. Chem. B* **2002**, *106*, 325–333.
21. Rothenberger, G.; Fitzmaurice, D.; Grätzel, M. Spectroscopy of Conduction Band Electrons in Transparent Metal Oxide Semiconductor Films: Optical Determination of the Flatband Potential of Colloidal Titanium Dioxide Films. *J. Phys. Chem.* **1992**, *96*, 5983–5986.
22. Tachibana, Y.; Moser, J. E.; Grätzel, M.; Klug, D. R.; Durrant, J. R. Subpicosecond Interfacial Charge Separation in Dye-Sensitized Nanocrystalline Titanium Dioxide Films. *J. Phys. Chem.* **1996**, *100*, 20056–20062.
23. Moser, J. E.; Noukakis, D.; Bach, U.; Tachibana, Y.; Klug, D. R.; Durrant, J. R.; Humphry-Baker, R.; Grätzel, M. Comment on "Measurement of Ultrafast Photoinduced Electron Transfer from Chemically Anchored Ru-Dye Molecules into Empty Electronic States in a Colloidal Anatase TiO_2 Film. *J. Phys. Chem. B* **1998**, *102*, 3649–3650.
24. Kelly, C. A.; Farzad, F.; Thompson, D. W.; Stipkala, J. M.; Meyer, G. J. Cation-Controlled Interfacial Charge Injection in Sensitized Nanocrystalline TiO_2. *Langmuir* **1999**, *15*, 7047–7054.
25. Pelet, S.; Moser, J. E.; Grätzel, M. Cooperative Effect of Adsorbed Cations and Iodide on the Interception of Back Electron Transfer in the Dye Sensitization of Nanocrytalline TiO_2. *J. Phys. Chem. B* **2000**, *104*, 1791–1795.
26. Runge, E.; Gross, E. K. U. Density-Functional Theory for Time-Dependent Systems. *Phys. Rev. Lett.* **1984**, *52*, 997–1000.
27. Gross, E. K. U.; Kohn, W. Time-Dependent Density-Functional Theory. *Adv. Quantum Chem.* **1990**, *21*, 255–292.
28. Moser, J. E.; Wolf, M.; Lenzmann, F.; Grätzel, M. Photoinduced Charge Injection from Vibronically Hot Excited Molecules of a Dye Sensitizer into Acceptor States of Wide-Bandgap Oxide Semiconductors. *Z. Phys. Chem.* **1999**, *212*, 85–92.
29. Wang, P.; Zakeeruddin, S. M.; Moser, J.-E.; Grätzel, M. A New Ionic Liquid Electrolyte Enhances the Conversion Efficiency of Dye-Sensitized Solar Cells. *J. Phys. Chem. B* **2003**, *107*, 13280–13285.
30. Furube, A.; Katoh, R.; Hara, K.; Sato, T.; Murata, S.; Arakawa, H.; Tachiya, M. Lithium Ion Effect on Electron Injection from a Photoexcited Coumarin Derivative into a TiO_2 Nanocrystalline Film Investigated by Visible-to-IR Ultrafast Spectroscopy. *J. Phys. Chem. B* **2005**, *109*, 16406–16414.

31. Koops, S. E.; O'Regan, B. C.; Barnes, P. R.; Durrant, J. R. Parameters Influencing the Efficiency of Electron Injection in Dye-Sensitized Solar Cells. *J. Am. Chem. Soc.* **2009**, *131*, 4808–4818.
32. Morandeira, A.; López-Duarte, I.; O'Regan, B.; Martínez-Díaz, M. V.; Forneli, A.; Palomares, E.; Torres, T.; Durrant, J. R. Ru(II)-Phthalocyanine Sensitized Solar Cells: The Influence of Co-adsorbents upon Interfacial Electron Transfer Kinetics. *J. Mater. Chem.* **2009**, *19*, 5016–5026.
33. Katoh, R.; Kasuya, M.; Kodate, S.; Furube, A.; Fuke, N.; Koide, N. Effects of 4-*tert*-Butylpyridine and Li Ions on Photoinduced Electron Injection Efficiency in Black-Dye-Sensitized Nanocrystalline TiO_2 Films. *J. Phys. Chem. C* **2009**, *113*, 20738–20744.
34. Rühle, S.; Greenshtein, M.; Chen, S.-G.; Merson, A.; Pizem, H.; Sukenik, C. S.; Cahen, D.; Zaban, A. Molecular Adjustment of the Electronic Properties of Nanoporous Electrodes in Dye-Senstitized Solar Cells. *J. Phys. Chem. B* **2005**, *109*, 18907–18913.
35. Shalom, M.; Rühle, S.; Hod, I.; Yahav, S.; Zaban, A. Energy Level Alignment in CdS Quantum Dot Sensitized Solar Cells Using Molecular Dipoles. *J. Am. Chem. Soc.* **2009**, *131*, 9876–9877.
36. Heller, A. Conversion of Sunlight into Electrical Power and Photoassisted Electrolysis of Water in Photoelectrochemical Cells. *Acc. Chem. Res.* **1981**, *14*, 154–162.
37. O'Regan, B. C.; Lenzmann, F. Charge Transport and Recombination in a Nanoscale Interpenetrating Network of n-Type and p-Type Semiconductors: Transient Photocurrent and Photovoltage Studies of TiO_2/Dye/CuSCN Photovoltaic Cells. *J. Phys. Chem. B* **2004**, *108*, 4342–4350.
38. Bailes, M.; Cameron, P. J.; Lobato, K.; Peter, L. M. Determination of the Density and Energetic Distribution of Electron Traps in Dye-Sensitized Nanocrystalline Solar Cells. *J. Phys. Chem. B* **2005**, *109*, 15429–15435.
39. Kopidakis, N.; Neale, N. R.; Frank, A. J. Effect of an Adsorbent on Recombination and Band-Edge Movement in Dye-Sensitized TiO_2 Solar Cells: Evidence for Surface Passivation. *J. Phys. Chem. B* **2006**, *110*, 12485–12489.
40. Quintana, M.; Edvinsson, T.; Hagfeldt, A.; Boschloo, G. Comparison of Dye-Sensitized ZnO and TiO_2 Solar Cells: Studies of Charge Transport and Carrier Lifetime. *J. Phys. Chem. C* **2007**, *111*, 1035–1041.
41. Haque, S. A.; Tachibana, Y.; Willis, R. L.; Moser, J. E.; Grätzel, M.; Klug, D. R.; Durrant, J. R. Parameters Influencing Charge Recombination Kinetics in Dye-Sensitized Nanocrystalline Titanium Dioxide Films. *J. Phys. Chem. B* **2000**, *104*, 538–547.
42. Hay, P. J.; Wadt, W. R. *Ab Initio* Effective Core Potentials for Molecular Calculations. Potentials for K to Au Including the Outermost Core Orbitals. *J. Chem. Phys.* **1985**, *82*, 299–310.